Steady-State and Time-Dependent Fluorescence Quenching Studies of the Binding of Anionic Micelles to Polycation†

Akihito Hashidzume,* Katsunori Yoshida,‡ and Yotaro Morishima

Department of Macromolecular Science, Graduate School of Science, Osaka University, Toyonaka, Osaka 560-0043, Japan

Paul L. Dubin*

Department of Chemistry, Indiana University-Purdue University, Indianapolis, Indiana 46205-2820

Received: May 30, 2001

Soluble complex formation between poly(*N*-methyl-4-vinylpyridinium chloride) (QPVP) and mixed micelles of dodecyl octa(ethylene glycol) monoether ($C_{12}E_8$) and sodium dodecyl sulfate (SDS), driven by electrostatic interactions in water, was investigated by turbidimetric, quasielastic light scattering, and fluorescence techniques. The polymer−micelle interaction was monitored through quenching of fluorescence of pyrene probes solubilized in $C_{12}E_8$/SDS mixed micelles, the quenching occurring upon binding of the micelles to QPVP. Unlike the case in which fluorescence-labeled polyelectrolytes are employed in conjunction with quencher-carrying micelles to monitor polymer−micelle interactions, QPVP plays a dual role as a polycation to interact with anionic micelles and a quencher for fluorescence of a probe solubilized in the micelle. Thus, hydrophobic contribution from fluorescence labels, an additional complexity in the former case, can be eliminated by employing QPVP, making it possible to monitor polymer−micelle interactions without hydrophobic effects. The presence of a well-defined critical mole fraction of SDS (Y_c) at which a soluble polymer−micelle complex formation begins to occur was confirmed. The Y_c values determined by turbidimetric and fluorescence titrations were found to be in good agreement. Dynamic interactions of QPVP with pyrene-carrying $C_{12}E_8$/SDS mixed micelles were monitored by steady-state and time-dependent fluorescence quenching techniques. The charge on the micelle was varied systematically by varying the mole fraction of SDS (Y) in the mixed micelle. Steady-state and time-dependent fluorescence-quenching data were analyzed using, as a first approximation, a kinetic model proposed previously. The lifetime of the micelle bound to the polymer (i.e., the residence time) was estimated as a function of the micelle surface charge density and ionic strength. Results revealed that the residence time is a strong function of both Y and the ionic strength.

Introduction

Interactions between polyelectrolytes and oppositely charged micelles normally lead to macroscopic phase separation in water.[1] However, polyelectrolyte−micelle interactions may lead to the formation of stable equilibrium complexes if the electrostatic attractions are attenuated by proper adjustment of the polyion linear charge density (ξ), the micelle surface charge density (σ), or the ionic strength (μ). Under properly adjusted conditions, soluble complexes with dimensions between 1 and 10 times those of the polyelectrolyte may be formed.[2−6]

The interaction of micelles with oppositely charged polyelectrolytes strongly resembles the interaction of polyelectrolytes with other particles of similar size and charge, such as proteins[7−11] and dendrimers.[12−14] In all these cases, complex formation occurs when σ reaches an adequate level, and the magnitude of this value varies nearly directly with μ^a ($a \approx {}^1/_2$) and inversely with ξ. The appearance of the complexed state is sufficiently abrupt to enable the identification of a critical surface charge density (σ_c), so that the foregoing observations may be expressed as

$$\sigma_c \propto \xi^{-1}\kappa^b \tag{1}$$

where κ is the Debye−Hückel parameter. The value of b may depend somewhat on micelle curvature and polyelectrolyte charge density[15] but for strong polyelectrolytes in combination with small micelles is in the range of $1.0 < b < 1.4$.[15,16] The observation of such phase-transition-like behavior is consistent with theoretical predictions[17−21] and simulations.[22] On the other hand, the measured quantities, the departures of which from preassociation levels are thought to signal the onset of complex formation (vide infra), display changes that are never truly discontinuous but instead vary in abruptness depending on the polyelectrolyte−micelle system.

These soluble polymer−micelle complexes have been investigated by various characterization methods, including turbidimetry,[23−26] dynamic and static light scattering,[2−6] viscometry,[6,27] electrophoretic light scattering,[6] microcalorimetry,[28] dye-solubilization,[29,30] equilibrium dialysis,[2,31,32] and fluorescence.[33−36] Among these methods, fluorescence techniques are expected to provide a powerful tool to gain insight into the dynamics of polyelectrolyte−micelle interactions. Recently, we used a pyrene-labeled polyanion in conjunction with quencher-carrying mixed micelles to characterize the microscopic polyelectrolyte−micelle phase transition.[33−36] The intensity of the polyelectro-

† Part of the special issue "Noboru Mataga Festschrift".

‡ Current address: Shiseido Basic Research Center, 2-2-1 Hayabuchi, Tsuzuki, Yokohama 224-8558, Japan

10.1021/jp0120460 CCC: $22.00
Published on Web 10/13/2001

CHART 1

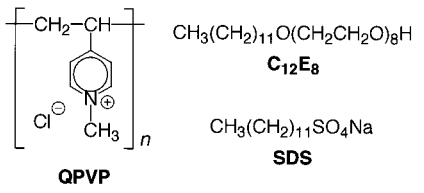

lyte−micelle interaction in such systems may be modulated by controlling the molar ratio of cationic and nonionic surfactants in the micelle (i.e., σ) and also by controlling the ionic strength (i.e., κ). The enhancement of quenching arising from dynamic interactions between a pyrene-labeled polyanion and quencher-carrying mixed micelles upon increase in σ or decrease in κ was investigated by steady-state and time-dependent fluorescence spectroscopy.[33−36] Of particular importance is kinetic information available from the latter technique. While the rate of change of, for example, light scattering or viscosity in the vicinity of "critical conditions" may be complicated by alterations in complex structure after binding per se, the measurement of micelle−polyion residence times at σ_c might provide more direct insight into the meaning of the observed transition-like behavior.

The behavior of fluorescence-labeled polyelectrolytes may be perturbed by the physicochemical properties of the label. Turbidimetric, light scattering, and fluorescence studies using a copolymer of sodium 2-(acrylamido)-2-methylpropanesulfonate (AMPS) (99 mol %) and *N*-(1-pyrenylmethyl)-methacrylate (PyMAm) (1 mol %), PyPAMPS, as a pyrene-labeled polyanion revealed that the interaction of PyPAMPS with mixed micelles of dodecyl hexa(ethylene glycol) monoether ($C_{12}E_6$) and cetyltrimethylammonium chloride (CTAC) occurred preferentially with pyrene sites, although the interaction was predominantly driven by electrostatic attractions.[33−35] These results indicate a conjoint effect of hydrophobic and electrostatic interactions on the polyion−micelle interaction.[33−35] The preferential binding of $C_{12}E_6$/CTAC mixed micelles to hydrophobic sites incorporated into a polyanion was confirmed in a systematic study using terpolymers of AMPS, PyMAm (1 mol %), and *N*-dodecylmethacrylamide (0−7.5 mol %) in conjunction with $C_{12}E_6$/CTAC mixed micelles in which cetylpyridinium chloride (CPC) is solubilized.[36] All of these results indicate that when fluorescence-labeled polyelectrolytes are employed to investigate the dynamics of the complex formation, the hydrophobic contributions from fluorescence-label sites are inevitable, although fluorescence quenching techniques are a powerful tool for studies of polyelectrolyte−micelle interactions.

To avoid hydrophobic contribution arising from fluorescence labels, we used poly(*N*-methyl-4-vinylpyridinium chloride) (QPVP) (Chart 1) as a polyelectrolyte to interact with mixed micelles of nonionic and anionic surfactants. Pyridinium cations are known to be an efficient quencher for singlet-excited pyrene by means of an electron-transfer mechanism.[37] Thus, QPVP is expected to play a dual role as a polycation and a quencher when the polymer interacts with pyrene-carrying micelles.

In this paper, we report on static and dynamic aspects of soluble complex formation between QPVP and mixed micelles of dodecyl octa(oxyethylene) glycol monoether ($C_{12}E_8$) and sodium dodecyl sulfate (SDS) (Chart 1) studied by means of turbidimetric titration, quasielastic light scattering, and fluorescence measurements in which molecular pyrene is solubilized in $C_{12}E_8$/SDS mixed micelles. A previously proposed kinetic model[35,36] was used to interpret steady-state and time-dependent fluorescence quenching data, which made it possible to examine the residence time of the micelle in the polymer−micelle complex as a function of the micelle charge density and the ionic strength. Such measurements may be directly comparable to the results of Monte Carlo simulations.[22]

Experimental Section

Materials. Poly(*N*-methyl-4-vinylpyridinium chloride) (QPVP) was prepared from poly(4-vinylpyridine) ($M_w = 7.7 \times 10^4$) obtained from Reilly Industries (Indianapolis).[38] Dodecyl octa(ethylene glycol) monoether ($C_{12}E_8$) (Nikko Chemical), purity confirmed by high performance liquid chromatography, was used as received. Sodium dodecyl sulfate (SDS) (Nakalai tesque) was recrystallized twice from methanol. Sodium chloride (NaCl) (Wako) was used without further purification. Milli-Q water was used for all experiments.

Turbidimetric Titration. Turbidimetric titrations were carried out at 450 nm with a Brinkmann PC800 probe colorimeter equipped with a 2 cm path length fiber optics probe. "Type 1" turbidimetric titrations[23−26] were performed at 25 ± 1 °C by adding an aqueous solution of 40 mM SDS at a constant ionic strength (μ) to a solution of 0.62 g/L (4 mM monomer units) QPVP and 20 mM $C_{12}E_8$ of the same μ. The values of μ were adjusted with NaCl. All transmittance values were corrected by subtracting the turbidity of a polymer-free blank. The blank-corrected turbidity (100 − %*T*) was plotted as a function of *Y*, the mole fraction of the anionic surfactant in the mixed micelle, defined as $Y = [SDS]/([C_{12}E_8] + [SDS])$. "Type 2" turbidimetric titrations[33,39,40] were carried out 25 ± 1 °C by adding an aqueous solution of 100 mM $C_{12}E_8$/SDS mixed micelle at a constant *Y* and a constant μ to a solution of 0.16 g/L (1 mM monomer units) QPVP of the same μ. The values of μ were adjusted with NaCl. The turbidity was plotted as a function of the concentration of total added surfactant (C_s).

Quasielastic Light Scattering (QELS). QELS measurements were carried out with a DynaPro 801 (Protein Solution Inc.), which employs a 30-mW solid-state 780-nm laser and an avalanche photodiode detector. Sample solutions were introduced into a 7-μL cell through a 0.1-μm Anotec filter. The 90° scattering data were analyzed employing cumulants to determine the apparent hydrodynamic radii (R_h). Sample solutions were prepared by adding a 40-mM SDS solution at a constant μ to a solution of 20 mM $C_{12}E_8$ and 0.62 g/L (4 mM monomer units) QPVP of the same μ.

Fluorescence. Steady-state fluorescence spectra were recorded on a Hitachi F-4500 fluorescence spectrophotometer with excitation at 338 nm.

A pyrene-carrying $C_{12}E_8$ micelle stock solution was prepared as follows: About 20 μL of an acetone solution of 13 mM pyrene was placed in a 20 mL volumetric flask. After evaporation of the solvent, pyrene was dissolved in $C_{12}E_8$ (647.9 mg, 1.20 mmol), and then a predetermined concentration of aqueous NaCl was added to the mixture. The solution was stirred overnight. The concentration of pyrene was determined by absorption spectroscopy using $\epsilon = 2.9 \times 10^4$ M^{-1} cm^{-1} determined for pyrene in 4:1 (v/v) ethanol/water.

For "type 1" fluorescence titration,[33−36] a solution of 40 mM SDS in a predetermined concentration of NaCl was added to a solution containing 0.62 g/L (4 mM monomer units) QPVP and 20 mM pyrene-tagged $C_{12}E_8$ at a constant ionic strength.

Fluorescence decays were measured by a time-correlated single-photon counting technique using a Horiba NAES 550 system. Decay curves were analyzed by a conventional decon-

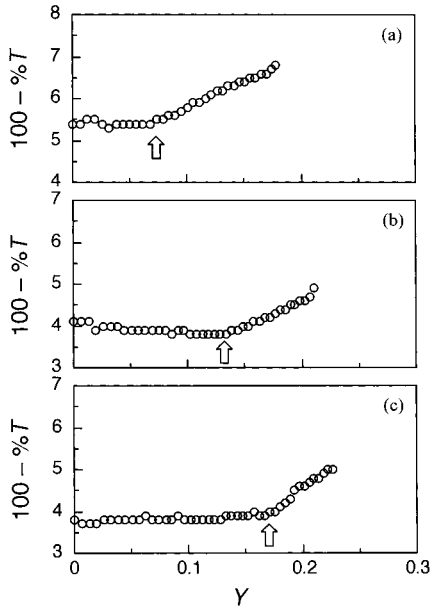

Figure 1. Type 1 turbidimetric titrations for 0.62 g/L (4 mM monomer units) QPVP and 20 mM $C_{12}E_8$ in 0.1 (a), 0.2 (b), and 0.3 M NaCl (c), using a 40 mM SDS solution of the same μ. The SDS solution was titrated to the mixed solution of the polymer and the micelle at a constant μ. Y is the mole fraction of SDS in the mixed micelle. Arrows denote Y_c values.

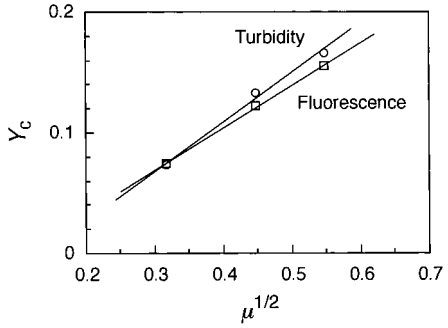

Figure 2. Dependence of Y_c, determined by turbidimetric and fluorescence titrations, on the square root of μ.

volution technique. Sample solutions were the same as those used for the steady-state fluorescence measurements described above.

Results and Discussion

Type 1 Turbidimetric Titrations. Solutions containing 0.62 g/L (4 mM monomer units) QPVP and 20 mM $C_{12}E_8$ were titrated with a 40-mM SDS aqueous solution at varying μ. Figure 1 shows the turbidity (reported as 100 − %T) as a function of Y (the mole fraction of SDS in $C_{12}E_8$/SDS mixed micelles). At $\mu = 0.1$, the turbidity is nearly constant in the region of $0 \leq Y \leq 0.07$ but it commences to increase at $Y = 0.07$, indicative of complex formation between QPVP and $C_{12}E_8$/SDS mixed micelles. This Y value is designated as Y_c. As μ is increased from 0.1 to 0.2 and 0.3, Y_c increases to 0.13 and 0.17, respectively. These observations are qualitatively consistent with those found for a number of polyelectrolyte−mixed micelle systems reported so far.[23−25,33,41,42] As shown in Figure 2, the dependence of Y_c on μ is roughly consistent with previous results for other polyelectrolyte−micelle systems.[24,33,42] The number of measurements at different μ is not large enough to specify the exact dependence of Y_c on μ, but the ionic strength effect does suggest that the QPVP−$C_{12}E_8$/SDS interaction is driven by electrostatic attractions.

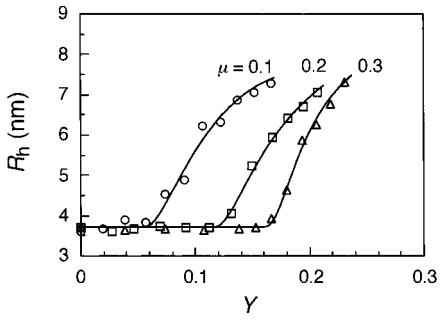

Figure 3. R_h as a function of Y at varying μ. Y values were adjusted by adding a 40 mM SDS solution to a solution containing 20 mM $C_{12}E_8$ and 0.62 g/L QPVP.

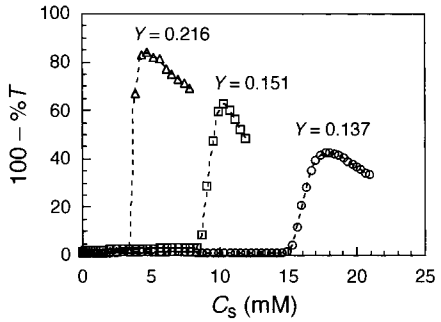

Figure 4. Type 2 turbidimetric titrations for 0.16 g/L (1 mM monomer units) QPVP in 0.1 M NaCl, using a 100 mM $C_{12}E_8$/SDS solution of the same μ. The solution of $C_{12}E_8$/SDS mixed micelles at a constant Y was titrated to the QPVP at $\mu = 0.1$. C_s is the total surfactant concentration.

QELS of the QPVP−$C_{12}E_8$/SDS System. QELS measurements were carried out to estimate the hydrodynamic size of QPVP−$C_{12}E_8$/SDS complexes. Y values were adjusted by adding a 40 mM SDS solution to a solution containing 20 mM $C_{12}E_8$ and 0.62 g/L QPVP. Figure 3 shows apparent values of R_h determined by cumulants as a function of Y at varying ionic strengths. At all ionic strengths studied, R_h values are nearly constant in the region of $Y < Y_c$.

Y_c values are estimated to be 0.06, 0.12, and 0.16 at $\mu = 0.1$, 0.2, and 0.3, respectively, i.e., consistently about 5−10% smaller than the turbidimetric estimates, possibly indicating the higher sensitivity of the QELS results. The increase in R_h for $Y \geq Y_c$ can arise either from a continuous increase in the size of complexes or from a shift in the population of scatterers, as the concentration of free micelles falls concomitant with an increase in the concentration of larger (but possibly uniform) complexes.

Type 2 Turbidimetric Titrations. Type 2 titrations, corresponding to the addition of mixed micelles at constant Y to polymer solution at constant μ, also provide information about the stoichiometry of complex formation. Type 2 turbidimetric titrations were conducted at 0.16 g/L QPVP + $C_{12}E_8$/SDS mixed micelles in 0.1, 0.2, and 0.3 M NaCl at constant Y. Figure 4 shows the results of the type 2 turbidimetric titrations at $\mu = 0.1$, in which the turbidity is plotted as a function of C_s. Even at a Y sufficiently higher than Y_c (0.07), turbidity shows only a slight increase with C_s in the lower C_s region. When C_s is further increased beyond a certain value, turbidity increases remarkably, indicative of phase separation. As Y is increased, the critical C_s decreases and the increase in turbidity at about the critical C_s becomes more abrupt. At $\mu = 0.2$ and 0.3, the tendencies are the same as that at $\mu = 0.1$. Because the soluble complexes are

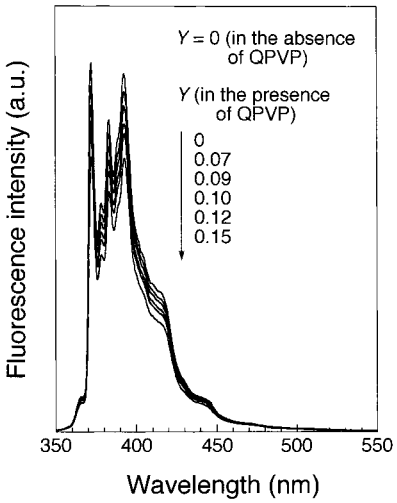

Figure 5. Fluorescence spectra of pyrene-carrying $C_{12}E_8$/SDS mixed micelles of varying Y in the absence and presence of QPVP in 0.1 M NaCl. Y values were adjusted by addition of 40 mM SDS in 0.1 M NaCl to a mixture of 0.62 g/L QPVP, 20 mM $C_{12}E_8$, and 4.6 μM pyrene.

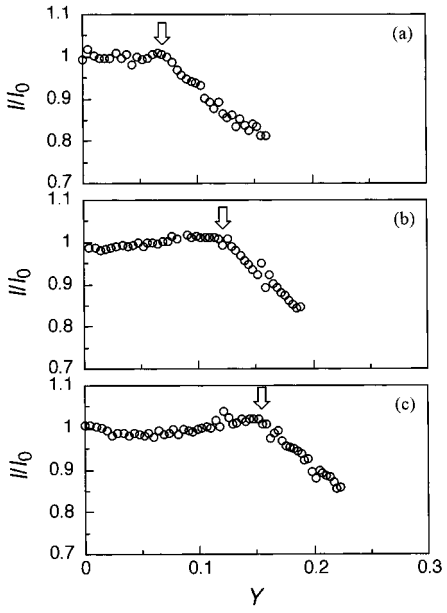

Figure 6. Type 1 fluorescence titration plots for solutions of 0.62 g/L (4 mM monomer units) QPVP and 20 mM $C_{12}E_8$ in 0.1 (a), 0.2 (b), and 0.3 M NaCl (c), using a 40 mM SDS solution of the same ionic strength as a titrant. Arrows denote Y_c values.

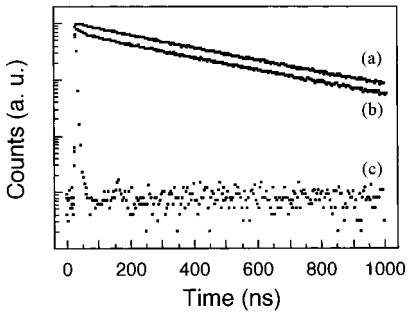

Figure 7. Fluorescence decay profiles for pyrene-carring $C_{12}E_8$/SDS mixed micelles of $Y = 0$ (a) and 0.174 (b) in the presence of QPVP at $\mu = 0.1$, accompanied by the lamp profile (c). Y values were adjusted by addition of 40 mM SDS in 0.1 M NaCl to a mixture of 0.62 g/L QPVP, 20 mM $C_{12}E_8$, and 4.6 μM pyrene.

intrapolymer at low C_s, the turbidity is small, indicating that soluble complexes are in association equilibrium even at a Y much higher than Y_c. Above the critical C_s, highly turbid interpolymer complexes are formed presumably because of charge neutralization of the complexes, resulting in phase separation.

Type 1 Fluorescence Titrations. To monitor the polymer−micelle interaction by fluorescence quenching, pyrene was dissolved in $C_{12}E_8$/SDS micelles and fluorescence was monitored in the presence of QPVP as a function of Y. Figure 5 shows fluorescence spectra of pyrene solubilized in $C_{12}E_8$/SDS mixed micelles of varying Y in the absence and the presence of QPVP in 0.1 M NaCl. Values of Y were adjusted by adding a 40 mM SDS solution to a mixture of 0.62 g/L QPVP, 20 mM $C_{12}E_8$, and 4.6 μM pyrene. Complete dissolution of pyrene in the micelle was confirmed by the fact that fluorescence decay is single-exponential with a lifetime of ca. 380 ns, as will be discussed in detail in the following subsection. Figure 5 shows a significant decrease in the fluorescence intensity with increasing Y, indicating that the fluorescence quenching occurs upon complex formation. Figure 6 shows the Y-dependence of the normalized fluorescence intensity, I/I_0, where I denotes the fluorescence intensity of the pyrene-carrying $C_{12}E_8$/SDS micelles at varying Y in the presence of QPVP and I_0 denotes the fluorescence intensity in the absence of QPVP at $Y = 0$. It was confirmed that in the absence of QPVP, the fluorescence intensity was independent of Y, i.e., the fluorescence intensity remains unchanged after adding SDS to pyrene-carrying $C_{12}E_8$ micelles (data not shown). At $\mu = 0.1$, fluorescence intensities at $Y \leq 0.07$ are virtually the same as I_0. Fluorescence quenching is only observed at $Y > 0.07$, and the extent of the quenching increases as Y is increased. These observations provide evidence for the complex formation of QPVP with the pyrene-carrying micelle at $Y \geq Y_c$ and an increase in the fraction of bound micelles with increasing micellar charge density. From the results of fluorescence quenching, Y_c values were determined to be 0.07, 0.12, and 0.16 at $\mu = 0.1$, 0.2, and 0.3, respectively. As shown in Figure 2, these Y_c values are in good agreement with those determined by turbidimetric titration.

After Y_c is reached, quenching increases gradually and almost linearly with further increase in Y. The same behavior is reflected in Figure 1, in which the turbidity increases gradually after Y_c is reached. Figures 1 and 3 show that the turbidity increase is correlated with an increase in complex size. Thus, all of these data show a progressive increase in complex formation, which could be a fundamental characteristic of these systems or might arise in part from some system polydispersity that reduces the sharpness of the transition. One such polydispersity could be the compositional variability of the mixed micelles, but rather little information is currently available on this point. Recent work on the polyelectrolyte-binding of a single-surfactant micelle system[15] suggests that a continuous increase in the binding constant beyond the critical micelle charge density is not limited to chemically mixed micelles but rather is characteristic of all related systems. For this reason, we describe the micelles to a first approximation only in terms of their average composition, i.e., the stoichiometric value of Y.

Time-Dependent Fluorescence Quenching for QPVP−$C_{12}E_8$/SDS. Figure 7 shows an example of typical fluorescence decay profiles for pyrene-carrying $C_{12}E_8$/SDS mixed micelles of $Y = 0$ and 0.174 in the presence of QPVP at $\mu = 0.1$. Decays are completely single-exponential when Y is small, but as Y is increased, decays are best-fitted to a double-exponential function. However, a Y value at which the transition occurs from

TABLE 1: Lifetimes Determined by Fitting Fluorescence Decay Profiles

μ	Y	τ_0[a] (ns)	τ_S (ns)	τ_L (ns)	χ^2
0.1	0	379		378	1.01
0.1	0.09	384	41.7	377	1.23
0.1	0.10	383	48.5	376	1.25
0.1	0.12	384	37.6	375	1.18
0.1	0.16	382	29.6	372	1.16
0.1	0.17	382	39.1	371	1.10
0.2	0	379		381	1.12
0.2	0.14	383	44.1	378	1.06
0.2	0.16	385	34.1	376	1.24
0.2	0.18	386	40.2	374	1.04
0.2	0.20	384	43.8	372	1.07
0.2	0.21	382	35.3	370	1.06
0.3	0	383		382	1.32
0.3	0.17	384	78.2	381	1.14
0.3	0.19	386	37.2	375	1.29
0.3	0.21	387	35.3	374	1.12
0.3	0.23	387	35.6	372	1.07
0.3	0.24	387	35.0	370	1.24

[a] The fluorescence lifetime for pyrene-carrying mixed micelles in the absence of the quencher.

SCHEME 1

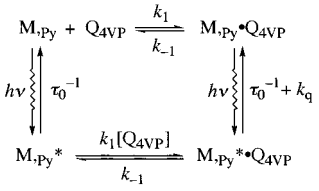

single- to double-exponential decay is not well-defined because, in the present system, fluorescence quenching efficiency is quite low. Above Y_c, however, we can assume that these decay profiles obey a double-exponential function, as suggested from our previous study with PyPAMPS−$C_{12}E_6$/CTAC interactions.[35] Thus, from the decay curves, the lifetimes of pyrene fluorescence were determined as shown in Table 1, where τ_S and τ_L denote the shorter and longer lifetimes, respectively. At each μ, τ_L decreases as Y is increased, although τ_S seems to be independent of Y.

Kinetic Analysis for Fluorescence Quenching. To quantitatively interpret the fluorescence quenching data, we use a kinetic model that we proposed in our earlier work.[35,36] This quenching model assumes an association equilibrium for the binding of pyrene-carrying $C_{12}E_8$/SDS mixed micelles to QPVP to form soluble complexes (Scheme 1). This assumtion is based on the observation that an association equilibrium is achieved in the region where soluble complexes are formed (Figure 4). Here, $M,_{Py}$ denotes the pyrene-carrying mixed micelles, Q_{4VP} denotes the pyridinium site in QPVP that acts as a quencher site, $M,_{Py}\cdot Q_{4VP}$ denotes the complex of $M,_{Py}$ with Q_{4VP}, k_1 and k_{-1} are the association and dissociation rate constants, respectively, τ_0 is the fluorescence lifetime of pyrene in the absence of the quencher, and k_q is the first-order rate constant for fluorescence quenching within the complex. In this model, it is assumed that all pyrene probes are completely solubilized in micelles and hence no pyrene molecules exist in the bulk water phase. When the system is irradiated with UV light at equilibrium, pyrene probes in both free (uncomplexed) and complexed micelles are photoexcited, fluorescence quenching occurring only in the complexed micelles. However, free micelles having photoexcited pyrene may encounter QPVP within its fluorescence lifetime to form a complex, which may be followed by quenching within the complex. Here, we assume that the rate of deactivation of singlet-excited pyrene in the complex is much faster than the rate of dissociation of the complex, that is $\tau_0^{-1} + k_q \gg k_{-1}$.

When the system is photoexcited by a light pulse at time $t = 0$, the total concentrations of the free and complexed micelles having photoexcited pyrene at time t are given by a double-exponential function with lifetimes τ_1 and τ_2 (eqs A4−A8 in Appendix). The reciprocals of these lifetimes are given by

$$(1/\tau_1) = (1/\tau_0) + k_q \tag{2}$$

and

$$(1/\tau_2) = (1/\tau_0) + k_1[Q_{4VP}] \tag{3}$$

On the other hand, the ratio of fluorescence quantum efficiencies in the presence and absence of QPVP is given by a function of τ_0, τ_1, τ_2, and $k_1[Q_{4VP}]$ (eq A12 in Appendix):

$$\Phi/\Phi_0 = \tau_1/\tau_0 + (\tau_2/\tau_0)(1 - \tau_1/\tau_0)\{1/(1 + K[Q_{4VP}])\} \tag{4}$$

On the basis of steady-state fluorescence data (Φ/Φ_0) and fluorescence decay data (τ_0, τ_1, and τ_2), one can calculate $K[Q_{4VP}]$ using eq 4. The quenching rate constant k_q and $k_1[Q_{4VP}]$ can be calculated from fluorescence decay data using eqs 2 and 3, respectively. From $K[Q_{4VP}]$ and $k_1[Q_{4VP}]$, the residence time $(1/k_{-1})$ of the micelle in the complex is calculated by

$$1/k_{-1} = K[Q_{4VP}]/k_1[Q_{4VP}] \tag{5}$$

The concentration of the pyridinium site that can actually act as a quencher site ($[Q_{4VP}]$) remains as an unknown parameter. Because the quencher sites are localized on the polymer chain, $[Q_{4VP}]$ should be much lower than the molar concentration of the pyridinium residue of QPVP present in the system. In general, polymer-bound quenchers behave as much less efficient quenchers than do the corresponding free quencher moieties. In the quenching event in the $M,_{Py}\cdot Q_{4VP}$ complex, there exist excess quencher sites in the complex for photoexcited pyrene to be completely quenched. However, the excess quencher sites act as charged sites to interact with micellar charge, the pyridinium site playing a dual role as quencher and binding sites.

We applied this kinetic model to the steady-state and time-dependent fluorescence data presented in Figure 6 and Table 1, in which τ_S and τ_L correspond to τ_1 and τ_2, respectively. This set of data suggests that quenching efficiency of QPVP is quite low as compared with our earlier work.[35,36] We confirmed that all pyrene probes (4.9 ± 0.7 μM) are completely solubilized in the $C_{12}E_8$ micelle (20 mM). Assuming that all pyrene probes are randomly distributed over the micelles according to a Poisson distribution, the average number of the probes solubilized in a micelle is calculated to be ca. 0.022 and the fraction of pyrene-carrying micelles to be ca. 0.022 ± 0.003. The rest of the micelles are pyrene-free. From the concentrations of the polymer (0.62 g/L) and $C_{12}E_8$ molecules (20 mM), along with the degree of polymerization for the polymer (ca. 730) and the aggregation number of the $C_{12}E_8$ micelle (ca. 90),[43] the ratio of the molar concentrations of the micelle and the polymer molecule, [micelle]/[polymer], is roughly calculated to be ca. 40, the micelle being in a large excess to the polymer molecule. This means that a considerable fraction of the polymers interact with pyrene-free micelles. This is another reason for the low quenching efficiency of QPVP. Moreover, the pyridinium sites may not be able to reach micelle cores where pyrene probes are solubilized because of an "excluded volume" effect between

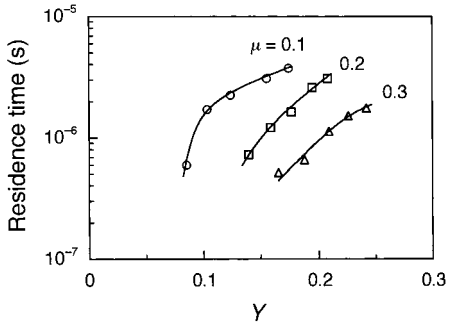

Figure 8. Plots of the residence time ($1/k_{-1}$) as a function of Y for the QPVP−$C_{12}E_8$/SDS system at $\mu = 0.1$, 0.2, and 0.3.

the polymer chain and the ethylene oxide corona layer of the mixed micelles. Such a situation would lead to a decreased quenching efficiency.

Using eqs A4−A6 (Appendix) and 2−5, we calculated the values of $1/k_{-1}$ at $\mu = 0.1$, 0.2, and 0.3 at varying Y. Results are plotted as a function of Y in Figure 8. The residence time depends strongly on both the micelle charge density and the ionic strength. For example, at $\mu = 0.1$, the residence time is ca. 0.6 μs at $Y = 0.09$ (at a Y slightly larger than Y_c), but it increases to ca. 3.8 μs at $Y = 0.17$, a 2-fold increase in the micelle charge density resulting in a more than 6-fold increase in the residence time. More dramatically, the residence time increases from ca. 0.5 to ca. 3.8 μs upon decrease in the ionic strength from 0.3 to 0.1, at $Y = 0.17$. This increase in residence time by almost an order of magnitude upon a 2-fold change in κ is consistent with the results of recent Monte Carlo simulations.[22,44] More dramatic effects may be expected with increasing colloid radius of curvature: Muthukumar[45] has obtained the result that the residence time for a polyelectrolyte on a flat oppositely charged surface decreases by over an order of magnitude with only a 50% increase in κ.

Our earlier work revealed an interplay of hydrophobic and electrostatic interactions in complexation of PyPAMPS with quencher-carrying mixed micelles of $C_{12}E_6$/CTAC.[35] Despite the presence of hydrophobic effects, the residence times were strongly dependent on micelle charge and ionic strength, and the residence times were on the same order as those measured here, for comparable conditions. This suggests that the contribution of pyrene interaction with micelles to the residence times might be a secondary effect in the PyPAMPS system.

Conclusions

To eliminate hydrophobic contribution from fluorescence labels attached to polyelectrolytes in interactions between fluorescence-labeled polyelectrolytes and surfactant micelles, we employed QPVP in conjunction with mixed micelles of $C_{12}E_8$ and SDS in which pyrene probes are solubilized. Interactions of QPVP with pyrene-carrying $C_{12}E_8$/SDS mixed micelles were investigated by turbidimetric, quasielastic light scattering, and steady-state and time-dependent fluorescence techniques. The critical mole fractions of SDS (Y_c), at which the formation of soluble polymer−micelle complexes starts to occur, were determined by turbidimetric and fluorescence techniques. The Y_c values determined by the two techniques are in good agreement. Dynamic interactions of QPVP with pyrene-carrying $C_{12}E_8$/SDS mixed micelles were investigated by steady-state and time-dependent fluorescence quenching techniques. The micelle charge density was varied systematically by varying the mole fraction of SDS (Y) in the mixed micelle. Through the use of a kinetic model that we proposed previously as a first approximation, steady-state and time-dependent fluorescence quenching data were analyzed to estimate the residence time (the lifetime of a polymer−micelle dynamic complex). Results indicate that the residence time is a strong function of Y and the ionic strength. In particular, a small decrease in the ionic strength causes a large increase in residence time.

Acknowledgment. P.D. acknowledges support from the National Science Foundation under Grant DMR0076068.

Appendix

According to Scheme 1, the concentration of the complex at equilibrium is given by

$$[\mathrm{M,_{Py}}\cdot\mathrm{Q_{4VP}}] = K[\mathrm{M,_{Py}}][\mathrm{Q_{4VP}}] \quad \text{(A1)}$$

where K is the association equilibrium constant (binding constant), i.e., $K = k_1/k_{-1}$.

Under transient conditions, the rate equations for $[\mathrm{M,_{Py}}^*]$ and $[\mathrm{M,_{Py}}^*\cdot\mathrm{Q_{4VP}}]$ with excitation at time $t = 0$ by a light pulse of negligible duration are given by

$$\mathrm{d}[\mathrm{M,_{Py}}^*]_t/\mathrm{d}t = -(\tau_0^{-1} + k_1[\mathrm{Q_{4VP}}])[\mathrm{M,_{Py}}^*]_t \quad \text{(A2)}$$

$$\mathrm{d}[\mathrm{M,_{Py}}^*\cdot\mathrm{Q_{4VP}}]_t/\mathrm{d}t = -(\tau_0^{-1} + k_q)[\mathrm{M,_{Py}}^*\cdot\mathrm{Q_{4VP}}]_t + k_1[\mathrm{M,_{Py}}^*]_t[\mathrm{Q_{4VP}}] \quad \text{(A3)}$$

Solving eqs A2 and A3 with the initial conditions of $[\mathrm{M,_{Py}}^*]_t = [\mathrm{M,_{Py}}^*]_{t=0}$ at $t = 0$ and $[\mathrm{M,_{Py}}^*\cdot\mathrm{Q_{4VP}}]_t = [\mathrm{M,_{Py}}^*\cdot\mathrm{Q_{4VP}}]_{t=0}$ at $t = 0$, the total concentrations of $[\mathrm{M,_{Py}}^*]$ and $[\mathrm{M,_{Py}}^*\cdot\mathrm{Q_{4VP}}]$ at time t are given by

$$[\mathrm{M,_{Py}}^*]_t + [\mathrm{M,_{Py}}^*\cdot\mathrm{Q_{4VP}}]_t = A\exp(-t/\tau_1) + B\exp(-t/\tau_2) \quad \text{(A4)}$$

where

$$A = [\mathrm{M,_{Py}}^*\cdot\mathrm{Q_{4VP}}]_{t=0}\{1 - k_{-1}/(k_q - k_1[\mathrm{Q_{4VP}}])\} \quad \text{(A5)}$$

$$B = [\mathrm{M,_{Py}}^*]_{t=0}\{k_q/(k_q - k_1[\mathrm{Q_{4VP}}])\} \quad \text{(A6)}$$

$$(1/\tau_1) = (1/\tau_0) + k_q \quad \text{(A7)}$$

and

$$(1/\tau_2) = (1/\tau_0) + k_1[\mathrm{Q_{4VP}}] \quad \text{(A8)}$$

Under steady-state conditions, the rate equations are given by

$$\mathrm{d}[\mathrm{M,_{Py}}^*]_t/\mathrm{d}t = \{[\mathrm{M,_{Py}}]/([\mathrm{M,_{Py}}] + [\mathrm{M,_{Py}}\cdot\mathrm{Q_{4VP}}])\}I_a - (\tau_0^{-1} + k_1[\mathrm{Q_{4VP}}])[\mathrm{M,_{Py}}^*]_t \quad \text{(A9)}$$

$$\mathrm{d}[\mathrm{M,_{Py}}^*\cdot\mathrm{Q_{4VP}}]_t/\mathrm{d}t = \{[\mathrm{M,_{Py}}\cdot\mathrm{Q_{4VP}}]/([\mathrm{M,_{Py}}] + [\mathrm{M,_{Py}}\cdot\mathrm{Q_{4VP}}])\}I_a + k_1[\mathrm{Q_{4VP}}][\mathrm{M,_{Py}}^*]_t - (\tau_0^{-1} + k_q)[\mathrm{M,_{Py}}^*\cdot\mathrm{Q_{4VP}}]_t \quad \text{(A10)}$$

where I_a is the rate of light absorption. When $\mathrm{d}[\mathrm{M,_{Py}}^*]_t/\mathrm{d}t = 0$ and $\mathrm{d}[\mathrm{M,_{Py}}^*\cdot\mathrm{Q_{4VP}}]_t/\mathrm{d}t = 0$ are used, the total steady-state concentrations of $[\mathrm{M,_{Py}}^*]$ and $[\mathrm{M,_{Py}}^*\cdot\mathrm{Q_{4VP}}]$ are given by

$$[M,_{Py}{}^*]_S + [M,_{Py}{}^*\cdot Q_{4VP}]_S = \{[M,_{Py}]/([M,_{Py}] + [M,_{Py}\cdot Q_{4VP}])\} I_a\{(1 + K[Q_{4VP}])(\tau_0{}^{-1} + k_1[Q_{4VP}]) + k_q\}/\{(\tau_0{}^{-1} + k_1[Q_{4VP}])(\tau_0{}^{-1} + k_q)\} \quad (A11)$$

The ratio of fluorescence quantum efficiencies in the presence and absence of the quencher, Q_{4VP}, is given by

$$\Phi/\Phi_0 = \tau_1/\tau_0 + (\tau_2/\tau_0)(1 - \tau_1/\tau_0)\{1/(1 + K[Q_{4VP}])\} \quad (A12)$$

Note Added after ASAP Posting

This article was released ASAP on 10/13/2001 with minor errors in eq 1 and the text following eq 1. The correct version was posted on 10/19/2001.

References and Notes

(1) For reviews, see: (a) Tsuchida, E.; Abe, K. *Adv. Polym. Sci.* **1982**, *45*, 1. (b) Smid, J.; Fish, D. In *Encyclopedia of Polymer Science and Engineering*; Kroshwitz, J. I., Ed.; Wiley-Interscience: New York, 1988; Vol. 11, p 720.

(2) Xia, J.; Dubin, P. L.; Kim, Y. *J. Phys. Chem.* **1992**, *96*, 6805.

(3) Li, Y.; Dubin, P. L.; Dautzenberg, H.; Lück, U.; Hartmann, J.; Tuzar, Z. *Macromolecules* **1995**, *28*, 6795.

(4) Li, Y.; Xia, J.; Dubin, P. L. *Macromolecules* **1994**, *27*, 7049.

(5) Li, Y.; Dubin, P. L.; Havel, H. A.; Edwards, S. L.; Dautzenberg, H. *Langmuir* **1995**, *11*, 2486.

(6) Xia, J.; Zhang, H.; Rigsbee, D. R.; Dubin, P. L.; Shaikh, T. *Macromolecules* **1993**, *26*, 2759.

(7) Park, J. M.; Muhoberac, B. B.; Dubin, P. L.; Xia, J. *Macromolecules* **1992**, *25*, 290.

(8) Tsuboi, A.; Izumi, T.; Hirata, M.; Xia, J.; Dubin, P. L.; Kokufuta, E. *Langmuir* **1996**, *12*, 6295.

(9) Wen, Y.-p.; Dubin, P. L. *Macromolecules* **1997**, *30*, 7856.

(10) Mattison, K. W.; Dubin, P. L.; Brittain, I. J. *J. Phys. Chem. B* **1998**, *102*, 3830.

(11) Sato, T.; Mattison, K. W.; Dubin, P. L.; Kamachi, M.; Morishima, Y. *Langmuir* **1998**, *14*, 5430.

(12) Li, Y.; Dubin, P. L.; Spindler, R.; Tomalia, D. *Macromolecules* **1995**, *28*, 8426.

(13) Shah, G.; Dubin, P. L.; Kaplan, J. I.; Newkome, G. R.; Moorefield, C. N.; Baker, G. R. *J. Colloid Interface Sci.* **1996**, *183*, 397.

(14) Zhang, H.; Dubin, P. L.; Ray, J.; Manning, G. S.; Moorefield, C. N.; Newkome, G. R. *J. Phys. Chem. B* **1999**, *103*, 2347.

(15) Feng, X.; Dubin, P. L.; Kirton, G. *Macromolecules* **2001**, *34*, 6373.

(16) Zhang, H.; Ohbu, K.; Dubin, P. L. *Langmuir* **2000**, *16*, 9082.

(17) Wiegel, F. W. *J. Phys. A: Math. Gen.* **1977**, *10*, 299.

(18) Evers, O. A.; Fleer, G. J.; Scheutjens, J. M. H. M.; Lyklema, J. *J. Colloid Interface Sci.* **1986**, *111*, 446.

(19) Muthukumar, M. *J. Chem. Phys.* **1987**, *86*, 7230.

(20) Odijk, T. *Langmuir* **1991**, *7*, 1991.

(21) von Goeler, F.; Muthukumar, M. *J. Chem. Phys.* **1994**, *100*, 7796.

(22) (a) Muthukumar, M. *J. Chem. Phys.* **1995**, *103*, 4723. (b) Chodanowski, P.; Stoll, S. *Macromolecules* **2001**, *34*, 2320.

(23) Dubin, P. L.; Rigsbee, D. R.; McQuigg, D. W. *J. Colloid Interface Sci.* **1985**, *105*, 509.

(24) McQuigg, D. W.; Kaplan, J. I.; Dubin, P. L. *J. Phys. Chem.* **1992**, *96*, 1973.

(25) Dubin, P. L.; Oteri, R. *J. Colloid Interface Sci.* **1983**, *95*, 453.

(26) Dubin, P. L.; Rigsbee, D. R.; Gan, L. M.; Fallon, M. A. *Macromolecules* **1988**, *21*, 2555.

(27) Jones, M. N. *J Colloid Interface Sci.* **1967**, *23*, 36.

(28) Rigsbee, D. R.; Dubin, P. L. *Langmuir* **1996**, *12*, 1928.

(29) Sudbeck, E. A.; Dubin, P. L.; Curran, M. E.; Skelton, J. *J. Colloid Interface Sci.* **1991**, *142*, 512.

(30) Tokiwa, F.; Tujii, K. *Bull. Chem. Soc. Jpn.* **1973**, *46*, 2684.

(31) Fishman, M. L.; Eirich, F. R. *J. Phys. Chem.* **1971**, *75*, 3135.

(32) Shirahama, K. *Colloid Polym. Sci.* **1974**, *252*, 978.

(33) Yoshida, K.; Morishima, Y.; Dubin, P. L.; Mizusaki, M. *Macromolecules* **1997**, *30*, 6208.

(34) Mizusaki, M.; Morishima, Y.; Yoshida, K.; Dubin, P. L. *Langmuir* **1997**, *13*, 6941.

(35) Morishima, Y.; Mizusaki, M.; Yoshida, K.; Dubin, P. L. *Colloids Surf., A* **1999**, *147*, 149.

(36) Mizusaki, M.; Morishima, Y.; Dubin, P. L. *J. Phys. Chem. B* **1998**, *102*, 1908.

(37) Chu, D.-Y.; Thomas, J. K. *Macromolecules* **1984**, *17*, 2142.

(38) Poly(4-vinylpyridine) was quaternized by methyl iodide in sulfolane under an argon atmosphere to form poly(*N*-methyl-4-vinylpyridinium iodide). Because iodide may quench pyrene fluorescence, the iodide was exchanged to chloride as follows: the iodide was exchanged to perchlorate by using silver perchlorate, and then the perchlorate was exchanged to chloride by dialysis against dilute hydrochloric acid (pH = 2.0) and by using an anion-exchange resin.

(39) Dubin, P. L.; Davis, D. *Colloids Surf.* **1985**, *13*, 113.

(40) Dubin, P. L.; The, S. S.; McQuigg, D. W.; Chew, C. H.; Gan, L. M. *Langmuir* **1989**, *5*, 89.

(41) Dubin, P. L.; Chew, C. H.; Gan, L. M. *J. Colloid Interface Sci.* **1989**, *128*, 566.

(42) Yoshida, K.; Sokhakian, S.; Dubin, P. L. *J. Colloid Interface Sci.* **1998**, *205*, 257.

(43) van Os, N. M.; Haak, J. R.; Rupert, L. A. M. *Physico-Chemical Properties of Selected Anionic, Cationic and Nonionic Surfactants*; Elsevier: Amsterdam, 1993.

(44) Some simulations of polyelectrolyte−micelle complexes have identified structural features without observation of any phase-transition-like behavior: Wallin, T.; Linse, P. *Langmuir*, **1996**, *12*, 305; *J. Phys. Chem.* **1996**, *100*, 17873.

(45) M. Muthukumar, University of Massachusetts, Amherst, MA. Private communication, 1997.